

BABAR Results on the Decays $B \rightarrow K L^+ L^-$ and $B \rightarrow K^* L^+ L^-$

BaBar Collaboration

Presented at First International Conference on Flavor Physics and CP Violation
(FPCP 2002), 5/16/2002—5/18/2002, Philadelphia, PA, USA

Stanford Linear Accelerator Center, Stanford University, Stanford, CA 94309

Work supported by Department of Energy contract DE-AC03-76SF00515.

BABAR Results on the Decays $B \rightarrow K\ell^+\ell^-$ and $B \rightarrow K^*\ell^+\ell^-$

John J. Walsh
(on behalf of the *BABAR* Collaboration)
Istituto Nazionale di Fisica Nucleare
Sezione di Pisa
john.walsh@pi.infn.it

Abstract

We present preliminary results on a search for the rare decays $B \rightarrow K\ell^+\ell^-$ and $B \rightarrow K^*\ell^+\ell^-$ performed with the *BABAR* experiment at the PEP-II B Factory. The data set consists of approximately 60 million $\Upsilon(4S) \rightarrow B\bar{B}$ decays. We obtain the results:

$$\begin{aligned} \mathcal{B}(B \rightarrow K\ell^+\ell^-) &= (0.84_{-0.24-0.18}^{+0.30+0.10}) \times 10^{-6} \\ \mathcal{B}(B \rightarrow K^*\ell^+\ell^-) &< 3.5 \times 10^{-6} \text{ at } 90\% \text{ C.L.} \end{aligned} \quad (1)$$

1 Introduction

The flavor-changing neutral current decays $B \rightarrow K\ell^+\ell^-$ and $B \rightarrow K^*\ell^+\ell^-$ (where ℓ is understood to be an electron or a muon) proceed primarily via the one-loop diagrams, known as penguin and box diagrams. The Standard Model branching ratios are predicted to be quite small, on the order of 10^{-7} to 10^{-6} [1, 2]. However, significant enhancements to the branching ratios are obtained when considering extensions to the Standard Model, such as super-symmetry [1, 2]. Indeed, these channels are very interesting due to their sensitivity to New Physics.

The decay modes considered for this analysis are eight in number: $B^+ \rightarrow K^+\ell^+\ell^-$, $B^0 \rightarrow K_S^0\ell^+\ell^-$, $B^+ \rightarrow K^{*+}\ell^+\ell^-$ and $B^0 \rightarrow K^{*0}\ell^+\ell^-$, where $K^{*0} \rightarrow K^+\pi^-$, $K^{*+} \rightarrow K_S^0\pi^+$, $K_S^0 \rightarrow \pi^+\pi^-$, and ℓ is either an e or μ . Charge-conjugate modes are implied throughout this paper. The results contained herein are preliminary.

The data set used to in the analysis consists of 56.4 fb^{-1} of on-peak data, corresponding to about 60 million $B\bar{B}$ pairs produced. We do not discuss the *BABAR* apparatus here, details can be found in reference [3].

Two primary kinematic variables are used to extract the signal from the background. The energy substituted mass, $m_{ES}\sqrt{E_b^{*2} - (\sum_i \mathbf{p}_i^*)^2}$ and $\Delta E = \sum_i \sqrt{m_i^2 + \mathbf{p}_i^{*2}} - E_b^*$, where E_b^* is the beam energy in the e^+e^- rest (c.m.) frame, \mathbf{p}_i^* is the c.m. momentum of daughter particle i in the B meson candidate, and m_i is the mass of particle i . Signal events have m_{ES} near the B meson mass (resolution is about 2.5 MeV)

and ΔE near zero (resolution is channel dependent). The analysis was conducted “blind”, meaning that event selection criteria were optimized on simulated events, without looking at the data or the sidebands used to measure the background rates. Only after the all selection criteria were established were the data actually examined.

2 Analysis Strategy

The basic analysis strategy can be summarized rather succinctly. Kaon and lepton candidates are appropriately combined to form $K\ell^+\ell^-$ or $K^*\ell^+\ell^-$ candidates. Backgrounds are suppressed by designing explicit vetoes or combined variables that discriminate signal from background. Extensive use of control samples allows us to determine our efficiency for the signal directly from the data and to perform general quality checks of our simulation. Finally, the signal yield is extracted from a two-dimensional fit in the m_{ES} vs. ΔE plane. We now discuss in more detail these various steps in the analysis.

Candidates are reconstructed selecting pairs of opposite charge leptons and combining them with identified kaons. Electron-positron pairs that are consistent with $\gamma \rightarrow e^+e^-$ are explicitly vetoed. For $K^* \rightarrow K\pi$ decays, the pion candidate is required to be inconsistent with the kaon hypothesis. The invariant mass of the reconstructed K^* is required to be within 75 MeV/ c^2 of the mean $K^*(892)$ mass. K_S^0 candidates are reconstructed from oppositely charge tracks that form a good vertex displaced from the primary vertex by at least 1 mm.

Obtaining sufficient suppression of the background is essential when search attempting to measure such small branching ratios. We now discuss the different types of background source and the techniques employed to suppress them.

Continuum backgrounds Backgrounds from the continuum are suppressed using event shape variables, *e.g.*, ratio of second and zeroth Fox-Wolfram moments. The variables are optimally combined employing the Fisher Discriminant technique. Further details of the continuum suppression may be found in [4].

$B\bar{B}$ backgrounds Another composite variable, based on likelihood ratios, uses the lepton and B vertex probabilities and the missing energy in the event to discriminate against backgrounds coming from $B\bar{B}$ events. E_{miss} is particularly useful, since most of this background comes from semileptonic B decays, which usually have large missing energy.

Decays to charmonium A significant background comes from the decays $B \rightarrow J/\psi(\rightarrow \ell^+\ell^-)K^{(*)}$ and $B \rightarrow \psi(2S)(\rightarrow \ell^+\ell^-)K^{(*)}$, which have the same topologies as the signal events. Figure 1 shows the rather complex veto region employed to remove these events. The veto was designed not only to reject candidates candidates with $M_{\ell\ell}$ near the J/ψ mass, but also candidates where one of the leptons has radiated a

photon or has otherwise been poorly measured. In such cases, there is a correlation between $M_{\ell\ell}$ and ΔE , which accounts for the diagonal bands observed in the figure.

Peaking Backgrounds There is a small contribution from backgrounds that peak in the signal region such as $B \rightarrow D(\rightarrow K\pi)\pi$, where both pions are misidentified as muons. Events compatible with this hypothesis are vetoed and the small contribution surviving the veto is accounted for in the extraction of the signal.

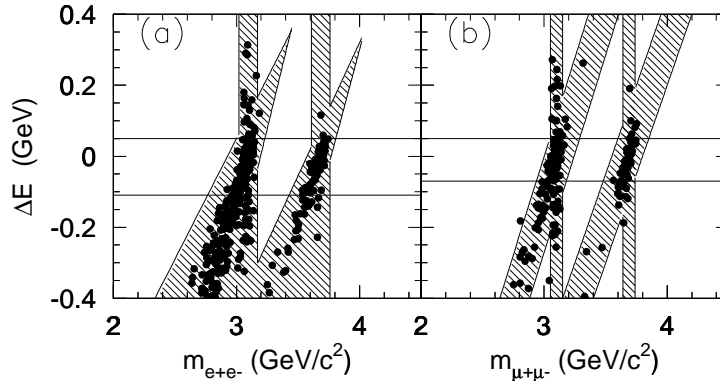


Figure 1: Regions in the ΔE - $M_{\ell\ell}$ plane employed to remove decays containing charmonium, (a) $B \rightarrow K^{(*)}e^+e^-$ decays and (b) $B \rightarrow K^{(*)}\mu^+\mu^-$ decays. Events falling in the hatched regions are removed from the analysis. The dots are simulated $B \rightarrow K J/\psi$ decays.

An important part of the analysis is the extensive use of control samples to validate our simulation and to derive our signal efficiency directly from the data. The most important control sample is comprised of charmonium decays, $B \rightarrow J/\psi(\rightarrow \ell^+\ell^-)K^{(*)}$ and $B \rightarrow \psi(2S)(\rightarrow \ell^+\ell^-)K^{(*)}$, that have been vetoed with the criteria discussed above. The J/ψ control sample has been used extensively to validate the Monte Carlo as well as to verify the efficiency for the signal obtained from the simulation. Combining all channels, the ratio of the efficiency obtained from the control sample to that obtained from the Monte Carlo is found to be 0.99 ± 0.02 . Additional control samples constructed from $Ke\mu$ combinations as well as combinations that fall far from the signal region (the Grand Sideband) in the m_{ES} - ΔE plane have also been used as checks on the simulation.

3 Results

The signal and background yields are obtained for each channel by performing a maximum likelihood fit in the region defined by $m_{ES} > 5.2 \text{ GeV}/c^2$ and $|\Delta E| < 0.25 \text{ GeV}$. The signal shapes, including radiation effects and correlations between ΔE and

m_{ES} , are taken from simulation. The background shape is a 2-dimensional ‘‘Argus’’ function, with two parameters which are determined directly from the fit. A small peaking background component is included in the background shape. The fit results are shown in Figure 2, which shows the projections of the fits onto the m_{ES} and ΔE axes. The fit yields for each mode are presented in Table 1.

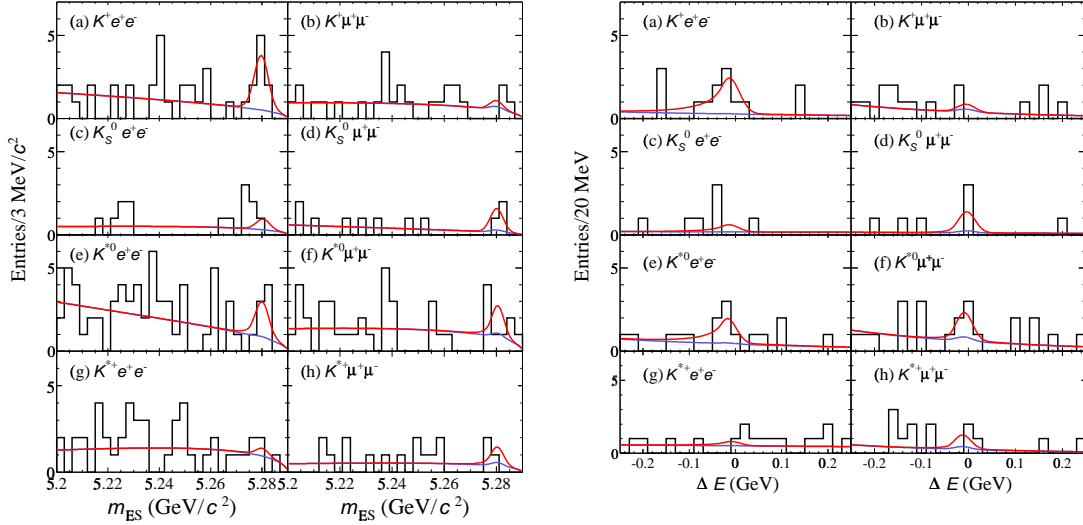


Figure 2: Projections of the two-dimensional fit, m_{ES} (left) and ΔE (right). The fit results are shown (both total fit and background contribution) are shown overlaid on the data.

Systematic uncertainties are divided into two categories, uncertainties on the efficiency, which are multiplicative in nature, and uncertainties on the yields from the fit procedure. The values are given, for each mode, in Table 1 in the columns labeled $(\Delta\mathcal{B}/\mathcal{B})_\epsilon$ and $(\Delta\mathcal{B})_{\text{fit}}$, respectively. The dominant uncertainties on the efficiency arise from the uncertainty on the charged tracking efficiency and from the theoretical model dependence of the efficiency. The main contributions to $(\Delta\mathcal{B})_{\text{fit}}$ come from uncertainties on the signal and background shapes in the fitting function.

The fit has all been performed combining the $K\ell^+\ell^-$ and $K^*\ell^+\ell^-$ modes together, with the results:

$$\begin{aligned}\mathcal{B}(B \rightarrow K\ell^+\ell^-) &= (0.84^{+0.30+0.10}_{-0.24-0.18}) \times 10^{-6} \\ \mathcal{B}(B \rightarrow K^*\ell^+\ell^-) &= (1.89^{+0.84}_{-0.72} \pm 0.31) \times 10^{-6}\end{aligned}\quad (2)$$

The theoretical constraint $\mathcal{B}(B \rightarrow K^*e^+e^-)/\mathcal{B}(B \rightarrow K^*\mu^+\mu^-) = 1.2$ from [1] has been employed for the combined fit.

Mode	Signal yield	Eff. bkgd	ϵ (%)	$(\Delta\mathcal{B}/\mathcal{B})_\epsilon$ (%)	$(\Delta\mathcal{B})_{\text{fit}}$ (10^{-6})	\mathcal{B} (10^{-6})
$B^+ \rightarrow K^+ e^+ e^-$	$9.6^{+4.6}_{-3.3}$	1.9	17.1	± 6.8	$^{+0.11}_{-0.23}$	$0.91^{+0.42+0.13}_{-0.32-0.24}$
$B^+ \rightarrow K^+ \mu^+ \mu^-$	$0.8^{+2.5}_{-1.3}$	1.2	9.9	± 6.8	± 0.10	$0.13^{+0.37}_{-0.23} \pm 0.10$
$B^0 \rightarrow K^0 e^+ e^-$	$1.8^{+2.8}_{-1.3}$	1.1	18.1	± 8.0	± 0.35	$0.47^{+0.69}_{-0.39} \pm 0.35$
$B^0 \rightarrow K^0 \mu^+ \mu^-$	$2.9^{+2.7}_{-1.3}$	0.4	10.3	± 7.8	± 0.22	$1.34^{+1.16}_{-0.78} \pm 0.25$
$B^0 \rightarrow K^{*0} e^+ e^-$	$7.3^{+4.7}_{-3.5}$	3.4	10.2	± 7.7	± 0.48	$1.66^{+1.08}_{-0.83} \pm 0.50$
$B^0 \rightarrow K^{*0} \mu^+ \mu^-$	$4.6^{+4.2}_{-2.9}$	2.3	6.6	± 9.3	± 0.39	$1.68^{+1.57}_{-1.09} \pm 0.42$
$B^+ \rightarrow K^{*+} e^+ e^-$	$1.5^{+4.0}_{-2.0}$	4.9	9.8	± 9.7	$^{+1.04}_{-1.06}$	$1.07^{+2.86+1.04}_{-1.51-1.06}$
$B^+ \rightarrow K^{*+} \mu^+ \mu^-$	$2.8^{+3.5}_{-2.0}$	1.5	5.4	± 11.1	± 1.82	$3.68^{+4.39}_{-2.88} \pm 1.86$

Table 1: Results from the fits to individual modes. The columns are, from left to right: fitted signal yield; the contribution of the background to the error on the signal yield, expressed as an effective background yield; the signal efficiency, ϵ (not including the branching fractions for K^* , K^0 , and K_s^0 decays); the systematic error on the selection efficiency, $(\Delta\mathcal{B}/\mathcal{B})_\epsilon$; the systematic error from the fit, $(\Delta\mathcal{B})_{\text{fit}}$; the branching fraction central value (\mathcal{B}); and the 90% C.L. upper limit on the branching fraction, including systematic uncertainties.

We have investigated the signal significance of the combined fit using a toy Monte Carlo technique and conclude that the $K\ell^+\ell^-$ signal is statistically significant at $> 5\sigma$ level. If systematic uncertainties are included, the significance remains above 4σ . The $K^*\ell^+\ell^-$ channel has a statistical significance of about 3.5σ and we choose to set an upper limit for that mode:

$$\mathcal{B}(B \rightarrow K^*\ell^+\ell^-) < 3.5 \times 10^{-6} \text{ at } 90\% \text{ C.L.}$$

4 Conclusions

We have analyzed the decay modes $B \rightarrow K\ell^+\ell^-$ and $B \rightarrow K^*\ell^+\ell^-$ in the *BABAR* experiment, with a data set of approximately 60 million $B\bar{B}$ events, and obtain the following results:

$$\begin{aligned} \mathcal{B}(B \rightarrow K\ell^+\ell^-) &= (0.84^{+0.30+0.10}_{-0.24-0.18}) \times 10^{-6} \\ \mathcal{B}(B \rightarrow K^*\ell^+\ell^-) &< 3.5 \times 10^{-6} \text{ at } 90\% \text{ C.L.} \end{aligned} \quad (3)$$

These results are compatible with *BABAR*'s previous $K\ell^+\ell^-/K^*\ell^+\ell^-$ results (upper limits for both modes) [4] at the few percent level and is consistent with Belle's recently published result [5].

All results presented in this paper are preliminary.

Acknowledgements

I would like to thank Prof. Nigel Lockyer and the other organizers of the *Flavor Physics-CP Violation Conference* for a very interesting and enjoyable conference.

References

- [1] A. Ali *et al.*, Phys. Rev. D **61**, 074024 (2000); P. Colangelo *et al.*, Phys. Rev. D **53**, 3672 (1996); D. Melikhov, N. Nikitin, and S. Simula, Phys. Rev. D **57**, 6814 (1998).
- [2] T.M. Aliev *et al.*, Phys. Lett. B **400**, 194 (1997); T.M. Aliev, M. Savci, and A. Özpineci, Phys. Rev. D **56**, 4260 (1997); G. Burdman, Phys. Rev. D **52**, 6400 (1995); C. Greub, A. Ioannissian, and D. Wyler, Phys. Lett. B **346**, 149 (1995); J.L. Hewett and J.D. Wells, Phys. Rev. D **55**, 5549 (1997); C.Q. Geng and C.P. Kao, Phys. Rev. D **54**, 5636 (1996); and references therein.
- [3] *BABAR* Collaboration, B. Aubert *et al.*, Nucl. Instrum. Methods **A479**, 1 (2002).
- [4] *BABAR* Collaboration, B. Aubert *et al.*, hep-ex/0201008, to be published in Phys. Rev. Lett. (2002).
- [5] Belle Collaboration, K. Abe *et al.*, Phys. Rev. Lett. **88**, 021801 (2002).